Computer Modeling in Engineering & Sciences

Tech Science Press

Doi:10.32604/cmes.2025.069023

ARTICLE

Hybrid Wavelet Methods for Nonlinear Multi-Term Caputo Variable-Order Partial Differential Equations

Junseo Lee[1], **Bongsoo Jang**[1] **and Umer Saeed**[1,2,*]

[1]Department of Mathematical Sciences, Ulsan National Institute of Science and Technology, Ulsan, 44919, Republic of Korea
[2]NUST Institute of Civil Engineering, School of Civil and Environmental Engineering, National University of Sciences and Technology (NUST), Sector H-12, Islamabad, 44000, Pakistan

*Corresponding Author: Umer Saeed. Email: umer.math@gmail.com

Received: 12 June 2025; Accepted: 30 July 2025; Published: 31 August 2025

ABSTRACT: In recent years, variable-order fractional partial differential equations have attracted growing interest due to their enhanced ability to model complex physical phenomena with memory and spatial heterogeneity. However, existing numerical methods often struggle with the computational challenges posed by such equations, especially in nonlinear, multi-term formulations. This study introduces two hybrid numerical methods—the Linear-Sine and Cosine (L1-CAS) and fast-CAS schemes—for solving linear and nonlinear multi-term Caputo variable-order (CVO) fractional partial differential equations. These methods combine CAS wavelet-based spatial discretization with L1 and fast algorithms in the time domain. A key feature of the approach is its ability to efficiently handle fully coupled space-time variable-order derivatives and nonlinearities through a second-order interpolation technique. In addition, we derive CAS wavelet operational matrices for variable-order integration and for boundary value problems, forming the foundation of the spatial discretization. Numerical experiments confirm the accuracy, stability, and computational efficiency of the proposed methods.

KEYWORDS: CAS wavelets; operational matrices; Caputo variable-order equations; exponential-sum-approximation; L1 approximation

1 Introduction

Wavelet theory has emerged as a powerful tool in numerical analysis due to its inherent ability to represent functions with localized features. Wavelets are a special kind of function that forms the basis of $L^2(\mathbb{R})$ and can be generated by dilating and translating a mother wavelet. They have a compact support that is, wavelets are zero outside a finite interval. This is the reason that wavelets-based operational matrices contain many zero entries. Researchers have worked on different wavelets for solving different types of fractional differential equations. Awati et al. [1] utilized the Haar wavelet-based collocation method and shifted Chebyshev collocation method for the simulations of magnetohydrodynamic flow of micropolar nanofluid with stagnation point model. Rabiei and Razzaghi [2] solve the fractional optimal control problems by using the fractional-order Boubaker wavelets method. Bernoulli wavelet operational matrix method [3] is used to solve the proposed glucose-insulin regulatory model. Neutral delay differential equations are solved by using the Gegenbauer and Bernoulli wavelets method in [4]. For more detail about the wavelet methods, we refer the readers to [5–7] and [8–11].

Parallel to this, fractional calculus—particularly with constant-order derivatives—has gained considerable attention over the past decade, owing to its capacity to model memory and hereditary properties in various scientific and engineering systems. Constant-order fractional calculus is the study of various types of fractional-order differential and integral operators. Variable-order (VO) fractional calculus is the generalization of the constant-order fractional calculus in which the order of its operators is a function of time or space or both. In recent years, VO differential equations have gained more interest among researchers due to their many applications in real world phenomena. The VO differential equations can more accurately describe the complex behavior of many physical phenomena. They enable a more precise depiction of nonlinear phenomena or systems experiencing abrupt changes. Like fractional differential and integral operators, there are many definitions of variable-order differential and integral operators with singular and non-singular kernel.

Despite the evident advantages of VO models, they have received comparatively less attention than their constant-order counterparts. We have reviewed several research articles from the literature which are focussed on the VO fractional calculus. For example, a Bernoulli polynomials-based method is proposed in [12] for solving multi-term VO ordinary differential equations in Caputo sense. Legendre wavelet based method is utilized in [13] for the solution of nonlinear VO ordinary differential equations. In [14], an explicit finite difference scheme is utilized for the solution of linear and semi-linear VO differential equations. The focus of the authors in [15] is to study the existence and uniqueness of weak solutions of VO Laplacian equations with variable exponents. In [16], authors present a method for the solution of Atangana-Baleanu VO mobile-immobile advection-dispersion model. Shen et al. [17] solve the VO time fractional diffusion equation by utilizing the L1 approximation for CVO fractional time derivative and the finite difference formula for the second-order spatial derivative. They have also worked on the analysis of the method.

Since the kernel of the VO fractional operators has a variable exponent, obtaining analytical solutions is difficult, and these have not gained much attention from the researchers. Building on these foundations, this paper aims to develop a robust numerical method for solving VO fractional differential equations by leveraging wavelet-based techniques. By integrating the localized efficiency of wavelets with the modeling flexibility of variable-order operators, we aim to contribute a more accurate and computationally efficient approach for complex nonlinear multi-term CVO partial differential equation of following form

$$\begin{aligned} {}^{C}D_t^{\gamma(s,t)}u(s,t) &= \sum_{j=1}^{J} a_j(s,t)\,{}^{C}D_s^{\beta_j(s,t)}u(s,t) + c(s,t)u(s,t) + g\big(u, {}^{C}D_s^{\alpha(s,t)}u\big) + f(s,t), \\ u(s,0) &= u_0(s),\ 0 \le s \le \eta,\ \eta \in \mathbb{R}^+, \\ u(0,t) = A_0(t),\ u(\eta,t) &= C_0(t),\ 0 \le t \le T,\ T \in \mathbb{R}^+, \end{aligned} \tag{1}$$

where $0 < n_\gamma \le \gamma(s,t) \le m_\gamma \le 1,\ 0 < \alpha(s,t), \beta_j(s,t) \le 2,\ J \in \mathbb{N}$, and $g(u, {}^{C}D_s^{\alpha(s,t)}u)$ is any nonlinear functional of u and ${}^{C}D_s^{\alpha(s,t)}u$. Here, ${}^{C}D_t^{\gamma(s,t)}u$ is a CVO fractional time derivative defined by

$${}^{C}D_t^{\gamma(s,t)}u(s,t) = \frac{1}{\Gamma(1-\gamma(s,t))}\int_0^t (t-\tau)^{-\gamma(s,t)}\frac{\partial}{\partial\tau}u(s,\tau)d\tau. \tag{2}$$

The CVO fractional space derivatives, ${}^{C}D_s^{\beta_j(s,t)}u(s,t)$, are defined similarly. We have reviewed several research articles related to the variable-order partial differential equations, we will mention a few of them here. We found that most of the authors [18–24] focussed their attention on only $\gamma(t),\ t \in (0,1)$, order time derivative but integer order space derivatives partial differential equations. Some authors [25–28] consider the $\gamma(s,t),\ 0 \le s \le \eta,\ t \in (0,1)$, order time derivative but integer order space derivatives.

In [29,30], authors focussed their intention on the solution of variable-order partial differential equations in both VO space, $\beta(s)$, and time, $\gamma(t)$, derivative. Since the above problem (1) is a nonlinear multi-term CVO fractional partial differential equation in which the orders of both space and time derivatives are the functions of both time and spatial variables. Numerical techniques for solving these Eq. (1) are still in the early stages of development. This is the reason that we focussed our intention on the development of more efficient and accurate methods for the solution of (1). Our major contributions to this work are as follows:

- Zhang et al. [18] developed an exponential-sum-approximation (ESA) technique for $\gamma(t),\ t \in (0,1)$, order time derivative, and utilized it for the solution of diffusion equations with VO time and integer order spatial derivative. We extended the ESA technique for $\gamma(s,t),\ 0 \le s \le \eta,\ 0 \le t \le T$. The purpose of this extension is to get a fast approximation of ${}^{C}D_{t}^{\gamma(s,t)}u(s,t)$.
- To the best of our knowledge, this work is the first to propose a hybrid strategy for Caputo-type fractional differential equations with variable-order derivatives in both time and space, combining an efficient ESA-based scheme for the time component with CAS wavelet operational matrices for handling nonlinear space variable-order derivatives.
- To handle the nonlinearities, we designed the interpolation technique for the above problem (1). The purpose of using the interpolation technique for the treatment of nonlinear terms is to reduce the computational costs of the methods as compared to the quasilinearization technique and Adomian polynomials.
- We proposed two efficient method, the $L1$-CAS method and the fast-CAS method, for the solution of (1), by uniting the $L1$ approximations or the ESA technique for ${}^{C}D_{t}^{\gamma(s,t)}u(s,t)$, CAS wavelet variable-order operational matrices for CVO space derivatives, ${}^{C}D_{s}^{\beta_1(s,t)}u(s,t)$, ${}^{C}D_{s}^{\beta_2(s,t)}u(s,t)$, $\cdots$, ${}^{C}D_{s}^{\beta_J(s,t)}u(s,t)$, and the interpolation technique for the treatment of nonlinearities, given in Section 3.
- We performed the theoretical analysis of the proposed methods and provided the numerical simulations to illustrate the theoretical results. The obtained numerical results are thoroughly examined through both tabular and graphical representations.

This paper is organized as follows: Section 2 provides the detail about the CAS wavelet, the function approximations by the CAS wavelet series, and the construction of its operational matrices of variable-order integration. In Section 3, we discuss the algorithms of the L1-CAS method, the fast-CAS method, and their extension to the nonlinear multi-term CVO partial differential equation. Section 4 is dedicated to conducting the analysis of the proposed methods. In Section 5, we present two numerical examples aimed at evaluating the efficiency, reliability, and accuracy of our methods. In Section 6, we conclude our work.

2 CAS Wavelets

The cosine and sine (CAS) wavelets represent a distinct category of wavelet basis functions, originating from the cosine and sine functions. The CAS wavelets possess orthogonality to each other, streamlining computations and improving function representation. The classical CAS wavelets for interval $[0,1)$ is defined as [31]

$$\psi_{p,q}(s) = \begin{cases} 2^{\frac{\nu}{2}} CAS_q\left(2^{\nu}s - p\right), & \frac{p}{2^{\nu}} \le s < \frac{p+1}{2^{\nu}}, \\ 0, & elsewhere, \end{cases}$$

The CAS wavelets for interval $[0, \eta)$ is given as

$$\psi_{p,q}(s) = \begin{cases} \sqrt{2^v \eta} CAS_q\left(\frac{2^v}{\eta} s - p\right), & \eta \frac{p}{2^v} \le s < \eta \frac{p+1}{2^v}, \\ 0, & elsewhere, \end{cases} \tag{3}$$

where $CAS_q(s) = \cos(2q\pi s) + \sin(2q\pi s)$, and $v = 0, 1, 2, \cdots$, and $p = 0, 1, 2, \cdots, 2^v - 1$, is the level of resolution and translation parameter, respectively, $q \in \mathbf{Z}$.

These wavelets for all integers v and p produce an orthonormal basis of $L_2(\mathbb{R})$. These wavelets have compact support, that is, they are zero outside $\left[\eta \frac{p-1}{2^v}, \eta \frac{p}{2^v}\right)$. These wavelets are valuable for approximating solutions to differential equations, especially in scenarios where conventional methods may be computationally demanding or unfeasible.

The CAS wavelets are orthonormal, that is,

$$\int_0^\eta \psi_{p,q}(s)\psi_{p,q'}(s)ds = \delta_{qq'},$$

which can be proved by using the transformation $t = \frac{s}{\eta}$ in [31,32].

2.1 Function Approximations

Since the CAS wavelets for all v and p forms an orthonormal basis of $L_2[0, \eta)$, therefore, any function $u(s) \in L_2[0, \eta)$ can be represented by the infinite series of the CAS wavelets as

$$u(s) = \sum_{p=0}^{\infty} \sum_{q \in \mathbf{Z}} l_{p,q} \psi_{p,q}(s).$$

We can use the finite sum of basis functions, $\psi_{p,q}(s)$, to approximate $u(s)$ as

$$u(s) \approx \sum_{p=0}^{2^v-1} \sum_{q=-Q}^{Q} l_{p,q} \psi_{p,q}(s) = \mathbf{L}^T \mathbf{\Psi}(s),$$

where $M = 2^v(2Q+1)$, $Q \in \mathbb{N}$, and $\mathbf{L}$ and $\Psi(s)$ are vectors of length $M \times 1$, which are given below:

$$\mathbf{L} = [l_{0,-Q}, l_{0,-Q+1}, \cdots, l_{0,Q}, l_{1,-Q}, l_{1,-Q+1}, \cdots, l_{1,Q}, \cdots, l_{2^v-1,-Q}, l_{2^v-1,-Q+1}, \cdots, l_{2^v-1,Q}]^T$$
$$\mathbf{\Psi}(s) = [\psi_{0,-Q}(s), \psi_{0,-Q+1}(s), \cdots, \psi_{0,Q}(s), \psi_{1,-Q}(s), \psi_{1,-Q+1}(s), \cdots,$$
$$\psi_{1,Q}(s), \cdots, \psi_{2^v-1,-Q}(s), \psi_{2^v-1,-Q+1}(s), \cdots, \psi_{2^v-1,Q}(s)]^T.$$

Expand the truncated series of the CAS wavelets at the collocation points, $s_k = \eta \frac{2k-1}{2M}$, $k = 1, 2, \cdots, M$, we get the CAS wavelets matrix $\mathbf{\Psi}_{M \times M}$ as

$$\mathbf{\Psi}_{M \times M} = \left[\mathbf{\Psi}(s_1), \mathbf{\Psi}(s_2), \cdots, \mathbf{\Psi}(s_M)\right].$$

For $\nu = 1,\ Q = 1,\ \eta = 2$, we get

$$\boldsymbol{\Psi}_{6\times 6} = \begin{pmatrix} -0.5176 & -1.4142 & 1.9319 & 0 & 0 & 0 \\ 0 & 0 & 0 & -0.5176 & -1.4142 & 1.9319 \\ 1.4142 & 1.4142 & 1.4142 & 0 & 0 & 0 \\ 0 & 0 & 0 & 1.4142 & 1.4142 & 1.4142 \\ 1.9319 & -1.4142 & -0.5176 & 0 & 0 & 0 \\ 0 & 0 & 0 & 1.9319 & -1.4142 & -0.5176 \end{pmatrix}.$$

2.2 Operational Matrices

In this section, our focus is on the construction of CAS wavelet operational matrices of variable-order fractional integration, which enable us to transform the CVO differential equation into a matrix form. Also, the purpose of constructing the operational matrices is to make the calculations fast, because operational matrices contain many zero entries.

The CAS wavelets operational matrix of variable-order integration

Let $\eta_0 = \eta\frac{p-1}{2^\nu}$ and $\eta_1 = \eta\frac{p}{2^\nu}$. Apply the fractional integral operator of order $\gamma(s) > 0$ on the CAS wavelets as

$$\begin{aligned} {}_0I_s^{\gamma(s)}\psi_{p,q}(s) &= \frac{1}{\Gamma(\gamma(s))}\int_0^s (s-\tau)^{\gamma(s)-1}\psi_{p,q}(\tau)d\tau,\ \eta_0 \le s < \eta_1, \\ &= \frac{\sqrt{2^\nu\eta}}{\Gamma(\gamma(s))}\int_{\eta_0}^s (s-\tau)^{\gamma(s)-1} CAS_q\Big(\frac{2^\nu}{\eta}\tau - (p-1)\Big)d\tau, \\ &= \frac{\sqrt{2^\nu\eta}}{\Gamma(\gamma(s))}\Bigg(\int_{\eta_0}^s (s-\tau)^{\gamma(s)-1}\cos\Big(2^{\nu+1}\frac{q\pi}{\eta}\tau - 2q\pi(p-1)\Big)d\tau \\ &\quad + \int_{\eta_0}^s (s-\tau)^{\gamma(s)-1}\sin\Big(2^{\nu+1}\frac{q\pi}{\eta}\tau - 2q\pi(p-1)\Big)d\tau\Bigg). \end{aligned} \tag{4}$$

Let us denote ${}_0I_s^{\gamma(s)}\psi_{p,q}(s) = F_{p,q}^{\gamma(s)}(s),\ p = 0,1,2,\cdots,2^\nu - 1,\ q = \{-Q, -Q+1, \cdots, Q\},\ Q \in \mathbb{N}$. We can compute (4) by using the global adaptive technique command, "integral", at different values of the parameters p and q in MATLAB. In vector form, we can represent (4) as

$$\begin{aligned} \mathbf{F}^{\gamma(s)}(s) = [&F_{0,-Q}^{\gamma(s)}(s), F_{0,-Q+1}^{\gamma(s)}(s), \cdots, F_{0,Q}^{\gamma(s)}(s), F_{1,-Q}^{\gamma(s)}(s), F_{1,-Q+1}^{\gamma(s)}(s), \cdots, F_{1,Q}^{\gamma(s)}(s), \\ &\cdots, F_{2^\nu-1,-Q}^{\gamma(s)}(s), F_{2^\nu-1,-Q+1}^{\gamma(s)}(s), \cdots, F_{2^\nu-1,Q}^{\gamma(s)}(s)]^T. \end{aligned} \tag{5}$$

To get the CAS wavelets operational matrix of variable-order integration, we will expand (5) at the collocation points, $s_k = \eta\frac{2k-1}{2M},\ k = 1,2,\cdots,M$, as

$$\mathbf{F}_{M\times M}^{\gamma(s)} = \Big[\mathbf{F}^{\gamma(s_1)}(s_1), \mathbf{F}^{\gamma(s_2)}(s_2), \cdots, \mathbf{F}^{\gamma(s_M)}(s_M)\Big]. \tag{6}$$

For $\gamma(s) = \sin(s) + \exp(-s) - \frac{1}{2},\ \nu = 1,\ Q = 1,\ \eta = 2$, we obtain

$$\mathbf{F}_{6\times 6}^{\gamma(s)} = \begin{pmatrix} 0.0769 & -0.8856 & -0.0435 & 0.1269 & 0.0638 & 0.0479 \\ 0 & 0 & 0 & 0.1000 & -0.7268 & 0.0265 \\ 0.6368 & 1.0562 & 1.3831 & 1.3129 & 1.1350 & 0.8973 \\ 0 & 0 & 0 & 0.4173 & 0.9403 & 1.4072 \\ 0.8539 & 0.2597 & -0.3951 & -0.0572 & -0.0407 & -0.0338 \\ 0 & 0 & 0 & 0.5527 & 0.3749 & -0.4454 \end{pmatrix}.$$

The CAS wavelets operational matrix of variable-order integration for boundary value problems

To effectively solve the boundary value problems, it is mandatory to utilize another important operational matrix of variable order integration. To get this matrix, let us apply the $\gamma(s)$ order integral on (3) from 0 to η as

$$\begin{aligned} {}_0I_{\eta}^{\gamma(s)}\psi_{p,q}(s)|_{s=\eta} &= \frac{1}{\Gamma(\gamma(\eta))}\int_0^{\eta}(\eta-\tau)^{\gamma(\eta)-1}\psi_{p,q}(\tau)d\tau, \\ &= \frac{\sqrt{2^{\nu}\eta}}{\Gamma(\gamma(\eta))}\left(\int_{\eta_0}^{\eta_1}(\eta-\tau)^{\gamma(\eta)-1}\cos\left(2^{\nu+1}\frac{q\pi}{\eta}\tau - 2q\pi(p-1)\right)d\tau\right. \\ &\quad \left. + \int_{\eta_0}^{\eta_1}(\eta-\tau)^{\gamma(\eta)-1}\sin\left(2^{\nu+1}\frac{q\pi}{\eta}\tau - 2q\pi(p-1)\right)d\tau\right). \end{aligned} \tag{7}$$

Let us denote ${}_0I_{\eta}^{\gamma(s)}\psi_{p,q}(s)|_{s=\eta} = b_{p,q}^{\gamma(\eta)},\quad \gamma(\eta) > 0,\quad p = 0,1,2,\cdots,2^{\nu}-1,\quad q = [-Q, -Q+1, \cdots, 0, 1, \cdots, Q-1, Q],\ Q \in \mathbb{N}$. In vector form, we can represent (7) as

$$\mathbf{B}_{M\times 1}^{\gamma(\eta)} = [b_{0,-Q}^{\gamma(\eta)}, b_{0,-Q+1}^{\gamma(\eta)}, \cdots, b_{0,Q}^{\gamma(\eta)}, b_{1,-Q}^{\gamma(\eta)}, b_{1,-Q+1}^{\gamma(\eta)}, \cdots, b_{1,Q}^{\gamma(\eta)}, \cdots, b_{2^{\nu}-1,-Q}^{\gamma(\eta)}, b_{2^{\nu}-1,-Q+1}^{\gamma(\eta)}, \cdots, b_{2^{\nu}-1,Q}^{\gamma(\eta)}]^T.$$

Since $\mathbf{B}_{M\times 1}^{\gamma(\eta)}$ does not depend on any variable, this means that for $s_k = \eta\frac{2k-1}{2M},\ k = 1,2,\cdots,M$, we get same $\mathbf{B}_{M\times 1}^{\gamma(\eta)}$ at each collocation points. Therefore, we have

$$\mathbf{B}_{M\times M}^{\gamma(\eta)} = \left[\mathbf{B}_{M\times 1}^{\gamma(\eta)}, \mathbf{B}_{M\times 1}^{\gamma(\eta)}, \cdots, \mathbf{B}_{M\times 1}^{\gamma(\eta)}\right]. \tag{8}$$

For $\gamma(\eta) = \sin(\eta) + exp(-\eta) - \frac{1}{2},\ \nu = 1,\ Q = 1,\ \eta = 2$, we have

$$\mathbf{B}_{6\times 1}^{\gamma(\eta)} = \left[0.0415,\ 0.5879,\ 0.7300,\ 1.5917,\ -0.0300,\ 0.0752\right].$$

3 Algorithms

This section is devoted to the development of two methods, one is based on the fast algorithm and the CAS wavelet technique, and the second is based on the $L1$-approximations and the CAS wavelet technique for the solution of linear and nonlinear multi-term CVO fractional partial differential equations.

Consider the following general form of linear multi-term CVO fractional partial differential equation

$$\begin{aligned} {}^{C}D_{t}^{\gamma(s,t)}u(s,t) &= \sum_{j=1}^{J} a_j(s,t)\ {}^{C}D_{s}^{\beta_j(s,t)}u(s,t) + c(s,t)u(s,t) + f(s,t), \\ u(s,0) &= u_0(s),\ 0 \le s \le \eta, \\ u(0,t) &= A_0(t),\ u(\eta,t) = C_0(t),\ 0 \le t \le T, \end{aligned} \tag{9}$$

where $0 < \beta_j(s,t) \le 2,\ 0 < \gamma(s,t) \le 1,\ J \in \mathbb{N}$, ${}^{C}D_{t}^{\gamma(s,t)}u(s,t)$ represents the CVO time derivative of order $\gamma(s,t)$ of $u(s,t)$. In this work, we will evaluate ${}^{C}D_{t}^{\gamma(s,t)}u(s,t)$ by the L1-approximation or the fast algorithm. For CVO space derivatives, ${}^{C}D_{s}^{\beta_1(s,t)}u(s,t),\ {}^{C}D_{s}^{\beta_2(s,t)}u(s,t), \cdots,\ {}^{C}D_{s}^{\beta_J(s,t)}u(s,t)$, we will utilize the CAS wavelet technique.

3.1 The Fast-CAS Method

In this subsection, we will work to save the memory and computational time by constructing an efficient algorithm for the CVO time derivative, ${}^{C}D_{t}^{\gamma(s,t)}u(s,t),\ 0 < \gamma(s,t) \le 1$, and utilizing the CAS wavelet operational matrices technique. Discretize the time domain $[0,T],\ T \in \mathbb{R}^{+}$ as $t_r = r\Delta t,\ r = 0,1,2,\cdots,R \in \mathbb{N}$, and $\Delta t = \frac{T}{R}$. For space domain $[0,\eta],\ \eta \in \mathbb{R}^{+}$, we have $s_k = \eta\frac{2k-1}{2M},\ k = 1,2,\cdots,M$. Consider the CVO time derivative (2) at (s_k,t_r) and split it in terms of local and history part, we have

$${}^{C}D_{t}^{\gamma(s_k,t_r)}u(s_k,t_r) = H_{k,r} + L_{k,r}, \tag{10}$$

where $H_{k,r} = \frac{1}{\Gamma(1-\gamma(s_k,t_r))}\int_{0}^{t_{r-1}}(t_r-\tau)^{-\gamma(s_k,t_r)}\frac{\partial}{\partial\tau}u(s_k,\tau)d\tau$ and $L_{k,r} = \frac{1}{\Gamma(1-\gamma(s_k,t_r))}\int_{t_{r-1}}^{t_r}(t_r-\tau)^{-\gamma(s_k,t_r)}\frac{\partial}{\partial\tau}u(s_k,\tau)d\tau$ are called the history and local part, respectively. For $L_{k,r}$, we utilize the forward difference formula for the approximation of $\frac{\partial}{\partial\tau}u(s_k,\tau)$ on $[t_{r-1},t_r]$, and integrate the remaining part to have

$$L_{k,r} \approx \frac{u(s_k,t_r) - u(s_k,t_{r-1})}{\Delta t^{\gamma(s_k,t_r)}\Gamma(2-\gamma(s_k,t_r))}.$$

For $H_{k,r}$, we have

$$H_{k,r} = \frac{T^{-\gamma(s_k,t_r)}}{\Gamma(1-\gamma(s_k,t_r))}\int_{0}^{t_{r-1}}\left(\frac{t_r-\tau}{T}\right)^{-\gamma(s_k,t_r)}\frac{\partial}{\partial\tau}u(s_k,\tau)d\tau. \tag{11}$$

The kernel $\left(\frac{t_r-\tau}{T}\right)^{-\gamma(s_k,t_r)}$ can be approximated by using the Lemma 2 of [18] as

$$\left|\left(\frac{t_r-\tau}{T}\right)^{-\gamma(s_k,t_r)} - \sum_{i=N_l+1}^{N_U}\Omega_{k,r,i}e^{-\xi_i\left(\frac{t_r-\tau}{T}\right)}\right| \le \left(\frac{t_r-\tau}{T}\right)^{-\gamma(s_k,t_r)}\epsilon$$

where the quadrature weights and exponents are properly chosen by following the procedure [18,33], and are given as

$$\Omega_{k,r,i} = \frac{he^{\gamma(s_k,t_r)ih}}{\Gamma(\gamma(s_k,t_r))},\ \xi_i = e^{ih},\ \epsilon = \left(\frac{\Delta t}{T}\right)^{2},$$

$$h = \frac{2\pi}{\log(3) + m_\gamma\log(1/\cos 1) + \log(1/\epsilon)},$$

$$N_l = \left\lceil \frac{1}{hn_\gamma} \left(\log(\epsilon) + \log(\Gamma(1+m_\gamma)) \right) \right\rceil,$$
$$N_U = \left\lfloor \frac{1}{h} \left(\log\left(\frac{T}{\Delta t}\right) + \log(\log(1/\epsilon)) + \log(n_\gamma) + 0.5 \right) \right\rfloor, \tag{12}$$

where $0 < n_\gamma \le \gamma(s,t) \le m_\gamma \le 1$. Then the Eq. (11) can be written as

$$H_{k,r} \approx \frac{T^{-\gamma(s_k,t_r)}}{\Gamma(1-\gamma(s_k,t_r))} \sum_{i=N_l+1}^{N_U} \Omega_{k,r,i} V_{k,r,i},$$

where $V_{k,r,i} = \int_0^{t_{r-1}} e^{\xi_i(\frac{t_r-\tau}{T})} \frac{\partial}{\partial\tau} u(s_k,\tau) d\tau$. For $r=1$, $V_{k,1,i}=0$, and for $r=2,3,\cdots,R$, $V_{k,r,i}$ can be calculated by using the forward difference formula for $\frac{\partial}{\partial\tau}u(s_k,\tau)$, as

$$\begin{aligned} V_{k,r,i} &= \int_0^{t_{r-2}} e^{\xi_i(\frac{t_r-\tau}{T})} \frac{\partial}{\partial\tau} u(s_k,\tau) d\tau + \int_{t_{r-2}}^{t_{r-1}} e^{\xi_i(\frac{t_r-\tau}{T})} \frac{\partial}{\partial\tau} u(s_k,\tau) d\tau, \\ &\approx e^{-\xi_i\frac{\Delta t}{T}} V_{k,r-1,i} + \frac{u(s_k,t_{r-1}) - u(s_k,t_{r-2})}{\Delta t} \int_{t_{r-2}}^{t_{r-1}} e^{\xi_i(\frac{t_r-\tau}{T})} d\tau, \\ &= e^{-\xi_i\frac{\Delta t}{T}} V_{k,r-1,i} + T\frac{e^{-\xi_i\frac{\Delta t}{T}} - e^{-2\xi_i\frac{\Delta t}{T}}}{\xi_i \Delta t} \left(u(s_k,t_{r-1}) - u(s_k,t_{r-2}) \right). \end{aligned} \tag{13}$$

Substitute $H_{k,r}$ and $L_{k,r}$ in (10) to get the fast evaluation formula for the CVO time derivative of order $\gamma(s,t)$ as

$${}^F D_t^{\gamma(s_k,t_r)} u(s_k,t_r) = \frac{T^{-\gamma(s_k,t_r)}}{\Gamma(1-\gamma(s_k,t_r))} \sum_{i=N_l+1}^{N_U} \Omega_{k,r,i} V_{k,r,i} + \frac{u(s_k,t_r) - u(s_k,t_{r-1})}{\Delta t^{\gamma(s_k,t_r)} \Gamma(2-\gamma(s_k,t_r))}, \tag{14}$$

where $V_{k,r,i}$ is given in (13). For $r=1$, we have

$${}^F D_t^{\gamma(s_k,t_1)} u(s_k,t_1) = \frac{u(s_k,t_1) - u(s_k,t_0)}{\Delta t^{\gamma(s_k,t_1)} \Gamma(2-\gamma(s_k,t_1))}. \tag{15}$$

Let $e^r(s) = \frac{1}{\Delta t^{\gamma(s,t_r)}\Gamma(2-\gamma(s,t_r))}$, $a_j^r(s) = a_j(s,t_r)$ and $d^r(s) = c(s,t_r) - e^r(s)$. Utilize the fast algorithm (14) for the evaluation of Caputo variable-order time derivative, ${}^C D_t^{\gamma(s,t)} u(s,t)$, at $t = t_r$, $r = 1,2,3,\cdots,R$, in Eq. (9), we get

$$\begin{aligned} \sum_{j=1}^{J} a_j^r(s) {}^C D_s^{\beta_j(s,t_r)} u(s,t_r) + d^r(s) u(s,t_r) &= -f(s,t_r) - e^r(s) u(s,t_{r-1}) \\ &+ \frac{T^{-\gamma(s,t_r)}}{\Gamma(1-\gamma(s,t_r))} \sum_{i=N_l+1}^{N_U} \Omega_{s,r,i} V_{s,r,i}, \\ u(s,t_0) = u_0(s),\ u(0,t_r) = A_0(t_r),\ u(\eta,t_r) &= C_0(t_r), \end{aligned} \tag{16}$$

where $V_{s,r,i} = e^{-\xi_i \frac{\Delta t}{T}} V_{s,r-1,i} + T\frac{e^{-\xi_i \frac{\Delta t}{T}} - e^{-2\xi_i \frac{\Delta t}{T}}}{\xi_i \Delta t}\left(u(s,t_{r-1}) - u(s,t_{r-2})\right)$. Let

$$z_j^r(s) = \begin{cases} \dfrac{s^{1-\beta_j(s,t_r)}}{\eta\Gamma(2-\beta_j(s,t_r))}, & 0 < \beta_j(s,t_r) \le 1, \\ 0, & 1 < \beta_j(s,t_r) \le 2. \end{cases}$$

Apply the CAS wavelet technique on the semi discretized Eq. (16), along the boundary conditions. Firstly, we will approximate ${}^{C}D_s^2 u(s,t_r)$ by using the CAS wavelet series as

$${}^{C}D_s^2 u(s,t_r) \approx \sum_{p=0}^{2^{\nu}-1}\sum_{q=-Q}^{Q} l_{p,q}^r \psi_{p,q}(s). \tag{17}$$

Apply the Riemann-Liouville integral operator of order 2 on (17) and utilize the boundary conditions, we get

$$u(s,t_r) \approx \sum_{p=0}^{2^{\nu}-1}\sum_{q=-Q}^{Q} l_{p,q}^r \, {}_0I_s^2\psi_{p,q}(s) - \frac{s}{\eta}\sum_{p=0}^{2^{\nu}-1}\sum_{q=-Q}^{Q} l_{p,q}^r \, {}_0I_\eta^2\psi_{p,q}(\eta) + \frac{s}{\eta}(C_0(t_r) - A_0(t_r)) + A_0(t_r). \tag{18}$$

Now, apply the Caputo derivative of order $\beta_j(s,t_r)$ on (18) to get

$${}^{C}D_s^{\beta_j(s,t_r)} u(s,t_r) \approx \sum_{p=0}^{2^{\nu}-1}\sum_{q=-Q}^{Q} l_{p,q}^r \, {}_0I_s^{2-\beta_j(s,t_r)}\psi_{p,q}(s) - z_j^r(s)\sum_{p=0}^{2^{\nu}-1}\sum_{q=-Q}^{Q} l_{p,q}^r \, {}_0I_\eta^2\psi_{p,q}(\eta) + z_j^r(s)(C_0(t_r) - A_0(t_r)). \tag{19}$$

Let $e_r'(s) = \frac{s}{\eta}d^r(s)$, $o_j^r(s) = a_j^r(s)z_j^r(s)$ and $g_J^r(s) = -\left(\sum_{j=1}^{J} a_j^r(s)z_j^r(s) + e_r'(s)\right)(C_0(t_r) - A_0(t_r)) - d^r(s)A_0(t_r) - f(s,t) - e^r(s)u(s,t_{r-1}) + \frac{T^{-\gamma(s,t_r)}}{\Gamma(1-\gamma(s,t_r))}\sum_{i=N_l+1}^{N_U}\Omega_{s,r,i}V_{s,r,i}$. Put the values of ${}^{C}D_s^{\beta_j(s,t_r)}u(s,t_r)$ and $u(s,t_r)$ from Eqs. (19) and (18), respectively, in (16) to get

$$\sum_{p=0}^{2^{\nu}-1}\sum_{q=-Q}^{Q} l_{p,q}^r\left(\sum_{j=1}^{J} a_j^r(s) \, {}_0I_s^{2-\beta_j(s,t_r)}\psi_{p,q}(s) - \left(\sum_{j=1}^{J} o_j^r(s) + e_r'(s)\right){}_0I_\eta^2\psi_{p,q}(\eta) + d^r(s) \, {}_0I_s^2\psi_{p,q}(s)\right) = g_J^r(s). \tag{20}$$

Let $y_j^r(s) = o_j^r(s) + \frac{e_r'(s)}{J}$. Evaluate (20) at the collocation points to obtain

$$\mathbf{L}_r^T\left(\sum_{j=1}^{J}\mathbf{A}_j^r\mathbf{F}_{M\times M}^{2-\beta_j(s)} + \mathbf{D}^r\mathbf{F}_{M\times M}^2 - \sum_{j=1}^{J}\mathbf{Y}_j^r\mathbf{B}_{M\times M}^2\right) = \mathbf{G}_J^r, \tag{21}$$

where $\mathbf{G}_J^r{}_{M\times 1} = [g_J^r(\eta\frac{1}{2M}), g_J^r(\eta\frac{3}{2M}), \cdots, g_J^r(\eta\frac{2M-1}{2M})]^T$, and the matrices $\mathbf{F}_{M\times M}^{2-\beta_j(s,t_r)}$, $\mathbf{F}_{M\times M}^2$, and $\mathbf{B}_{M\times M}^2$ are given in Section 2.2. The diagonal matrices $\mathbf{A}_j^r$, $\mathbf{D}^r$, and $\mathbf{Y}_j^r$ are given below:

$$\mathbf{A}_j^r = \begin{bmatrix} a_j^r(s_1) & 0 & \cdots & 0 \\ 0 & a_j^r(s_2) & \cdots & 0 \\ \vdots & \vdots & \ddots & \vdots \\ 0 & 0 & \cdots & a_j^r(s_M) \end{bmatrix}, \ \mathbf{D}^r = \begin{bmatrix} d^r(s_1) & 0 & \cdots & 0 \\ 0 & d^r(s_2) & \cdots & 0 \\ \vdots & \vdots & \ddots & \vdots \\ 0 & 0 & \cdots & d^r(s_M) \end{bmatrix},$$

$$\mathbf{Y}_j^r = \begin{bmatrix} y_j^r(s_1) & 0 & \cdots & 0 \\ 0 & y_j^r(s_2) & \cdots & 0 \\ \vdots & \vdots & \ddots & \vdots \\ 0 & 0 & \cdots & y_j^r(s_M) \end{bmatrix}.$$

Solve the system (21) to get $\mathbf{L}_r^T$ at each value of t_r and put it in (18) to get the approximate solution $u(s,t_r)$ at $t = t_r,\ r = 1,2,\cdots,R$. See Algorithm 1 for details.

Algorithm 1: The fast-CAS method

Given: $\gamma(s,t),\ \beta_j(s,t),\ u_0(s),\ A_0(t),\ C_0(t)$
Input: $\Omega_{k,r,i},\ \xi_i,\ h,\ \epsilon,\ N_l,\ N_U,\ s_k,\ t_r,\ \nu,\ Q,\ R,\ T$
Construct: $\mathbf{F}_{M\times M}^2,\ \mathbf{B}_{M\times M}^2$ by using Eqs. (6) and (8)
for $r = 1,2,\ldots,R$ **do**
  if $r = 1$ **then**
    $V_{k,r,i} \leftarrow 0$
  else if $r \geq 2$ **then**
    $V_{k,r,i} \leftarrow e^{-\xi_i\frac{\Delta t}{T}} V_{k,r-1,i} + T\frac{e^{-\xi_i\frac{\Delta t}{T}} - e^{-2\xi_i\frac{\Delta t}{T}}}{\xi_i \Delta t}\left(u(s_k,t_{r-1}) - u(s_k,t_{r-2})\right)$
  end if
  Calculate: $\mathbf{A}_j^r,\ \mathbf{D}^r,\ \mathbf{Y}_j^r$ and $\mathbf{G}_J^r$
  Construct: $\mathbf{F}_{M\times M}^{2-\beta_j(s,t_r)}$
  $\mathbf{L}_r^T \leftarrow \mathbf{G}_J^r\left(\sum_{j=1}^{J} \mathbf{A}_j^r \mathbf{F}_{M\times M}^{2-\beta_j(s)} + \mathbf{D}^r\mathbf{F}_{M\times M}^2 - \sum_{j=1}^{J}\mathbf{Y}_j^r\mathbf{B}_{M\times M}^2\right)^{-1}$
  $u(s,t_r) \leftarrow \sum_{p=0}^{2^\nu-1}\sum_{q=-Q}^{Q} l_{p,q}^r\, {}_0I_s^2\psi_{p,q}(s) - \frac{s}{\eta}\sum_{p=0}^{2^\nu-1}\sum_{q=-Q}^{Q} l_{p,q}^r\, {}_0I_\eta^2\psi_{p,q}(\eta) + \frac{s}{\eta}(C_0(t_r) - A_0(t_r)) + A_0(t_r)$
end for

3.2 The L1-CAS Method

To get the L1 approximation of (2), we evaluate (2) at (s,t_r) as

$${}^C D_t^{\gamma(s,t_r)} u(s,t_r) = \frac{1}{\Gamma(1-\gamma(s,t_r))}\int_0^{t_r} (t_r-\tau)^{-\gamma(s,t_r)}\frac{\partial}{\partial\tau}u(s,\tau)d\tau.$$

We will utilize the forward difference approximation to $\frac{\partial}{\partial\tau}u(s,\tau)$ over the interval $[t_j, t_{j+1}]$, $0 \le j \le r-1$ as $\frac{\partial}{\partial\tau}u(s,\tau) \approx \frac{u(s,t_{j+1})-u(s,t_j)}{\Delta t}$, we obtain

$$\begin{aligned}
{}^{L1}D_t^{\gamma(s,t_r)}u(s,t_r) &= \frac{1}{\Gamma(1-\gamma(s,t_r))}\sum_{j=0}^{r-1}\frac{u(s,t_{j+1})-u(s,t_j)}{\Delta t}\int_{t_j}^{t_{j+1}}(t_r-\tau)^{-\gamma(s,t_r)}d\tau,\\
&= \frac{\Delta t^{-\gamma(s,t_r)}}{\Gamma(2-\gamma(s,t_r))}\sum_{j=0}^{r-1}E_{j,r}(u(s,t_{j+1})-u(s,t_j)),\\
&\text{or}\\
&= \frac{\Delta t^{-\gamma(s,t_r)}}{\Gamma(2-\gamma(s,t_r))}\Big(E_{r-1,r}u(s,t_r)-\sum_{j=1}^{r-1}(E_{j,r}-E_{j-1,r})u(s,t_j)-E_{0,r}u(s,t_0)\Big),
\end{aligned} \tag{22}$$

where $E_{j,r} = (r-j)^{1-\gamma(s,t_r)} - (r-j-1)^{1-\gamma(s,t_r)}$, $r = 0, 1, \cdots, R$. Let $d^r(s) = c(s,t_r) - e^r(s)E_{r-1,r}$. Utilize the $L1$-approximation (22) for the evaluation of Caputo variable-order time derivative, ${}^{C}D_t^{\gamma(s,t)}u(s,t)$, at $t = t_r$, $r = 1, 2, 3, \cdots, R$, in Eq. (9), we get

$$\begin{aligned}
\sum_{j=1}^{J}a_j^r(s)\,{}^{C}D_s^{\beta_j(s,t_r)}u(s,t_r) + d^r(s)u(s,t_r) &= -f(s,t_r) - e^r(s)\sum_{i=1}^{r-1}(E_{i,r}-E_{i-1,r})u(s,t_i)\\
&\quad -e^r(s)E_{0,r}u(s,t_0),\\
u(s,t_0) = u_0(s),\ u(0,t_r) = A_0(t_r),\ u(\eta,t_r) &= C_0(t_r).
\end{aligned} \tag{23}$$

Let $y_j^r(s) = o_j^r(s) + \frac{e_r'(s)}{J}$ and $\omega_J^r(s) = -f(s,t_r) - e^r(s)\sum_{i=1}^{r-1}(E_{i,r}-E_{i-1,r})u(s,t_i) - e^r(s)E_{0,r}u(s,t_0) - \left(\sum_{j=1}^{J}y_j^r(s)\right)(C_0(t_r)-A_0(t_r)) - d^r(s)A_0(t_r)$. The second step is to apply the CAS wavelet technique on (23). For that purpose, we utilize the Eqs. (19) and (18) in Eq. (23) to get

$$\begin{aligned}
\sum_{p=0}^{2^v-1}\sum_{q=-Q}^{Q}l_{p,q}^r\Bigg(&\sum_{j=1}^{J}a_j^r(s)\,{}_0I_s^{2-\beta_j(s,t_r)}\psi_{p,q}(s) - \left(\sum_{j=1}^{J}y_j^r(s)\right){}_0I_\eta^2\psi_{p,q}(\eta)\\
&+d^r(s)\,{}_0I_s^2\psi_{p,q}(s)\Bigg) = \omega_J^r(s).
\end{aligned} \tag{24}$$

Evaluate (24) at the collocation points to obtain

$$\mathbf{L}_r^T\left(\sum_{j=1}^{J}\mathbf{A}_j^r\mathbf{F}_{M\times M}^{2-\beta_j(s,t_r)} - \sum_{j=1}^{J}\mathbf{Y}_j^r\mathbf{B}_{M\times M}^2 + \mathbf{D}^r\mathbf{F}_{M\times M}^2\right) = \mathbf{\Omega}_J^r, \tag{25}$$

where $\mathbf{A}_j^r$, $\mathbf{D}^r$, $\mathbf{Y}_j^r$ are given above, and $\mathbf{\Omega}_J^r{}_{M\times 1} = [\omega_J^r(\eta\frac{1}{2M}), \omega_J^r(\eta\frac{3}{2M}), \cdots, \omega_J^r(\eta\frac{2M-1}{2M})]^T$. Solve the system (25) to get $\mathbf{L}_r^T$ at each value of t_r and put it in (18) to getthe approximate solution $u(s,t_r)$ at $t = t_r$, $r = 1, 2, \cdots, R$. See Algorithm 2 for details.

Algorithm 2: The L1-CAS method

Given: $\gamma(s,t)$, $\beta_j(s,t)$, $u_0(s)$, $A_0(t)$, $C_0(t)$

Input: s_k, t_r, ν, Q, R, T

Construct: $\mathbf{F}^2_{M\times M}$, $\mathbf{B}^2_{M\times M}$ by using Eqs. (6) and (8)

for $r = 1, 2, \ldots, R$ **do**

$E_{j,r} \leftarrow (r-j)^{1-\gamma(s,t_r)} - (r-j-1)^{1-\gamma(s,t_r)}$

Calculate: $\mathbf{A}^r_j$, $\mathbf{D}^r$, $\mathbf{Y}^r_j$ and $\mathbf{\Omega}^r_J$

Construct: $\mathbf{F}^{2-\beta_j(s,t_r)}_{M\times M}$

$$\mathbf{L}^T_r \leftarrow \mathbf{\Omega}^r_J\left(\sum_{j=1}^{J}\mathbf{A}^r_j\mathbf{F}^{2-\beta_j(s)}_{M\times M} - \sum_{j=1}^{J}\mathbf{Y}^r_j\mathbf{B}^2_{M\times M} + \mathbf{D}^r\mathbf{F}^2_{M\times M}\right)^{-1}$$

$$u(s,t_r) \leftarrow \sum_{p=0}^{2^\nu-1}\sum_{q=-Q}^{Q} l^r_{p,q}\,{}_0I^2_s\psi_{p,q}(s) - \frac{s}{\eta}\sum_{p=0}^{2^\nu-1}\sum_{q=-Q}^{Q} l^r_{p,q}\,{}_0I^2_\eta\psi_{p,q}(\eta) + \frac{s}{\eta}(C_0(t_r) - A_0(t_r)) + A_0(t_r)$$

end for

3.3 Nonlinear Caputo Variable-Order Partial Differential Equations

The classical interpolation technique [34] is adopted for handling the nonlinear terms. The purpose of using the interpolation technique for the treatment of nonlinear terms is to reduce the computational costs of the method as compared to the quasilinearization technique [35] and Adomian polynomials [36]. The procedure for handling the nonlinear term $g(u, {}^CD_s^{\alpha(s,t)}u)$ is as follow. According to the methodology, we split the Eq. (1) in the following forms

$$\mathcal{L}(s,t) = g(u(s,t), {}^CD_s^{\alpha(s,t)}u(s,t)),$$

where $\mathcal{L}(s,t) = {}^CD_t^{\gamma(s,t)}u(s,t) - \sum_{j=1}^{J} a_j(s,t)\,{}^CD_s^{\beta_j(s,t)}u(s,t) - c(s,t)u(s,t) - f(s,t)$.

- For $r = 1$

  Predictor : $\mathcal{L}(s,t_1) = g(u(s,t_0), {}^CD_s^{\gamma(s,t_0)}u(s,t_0))$,

  we get predictor as $\bar{u}(s,t_1)$.

  Corrector : $\mathcal{L}(s,t_1) = g(\bar{u}(s,t_1), {}^CD_s^{\gamma(s,t)}\bar{u}(s,t_1))$,

  we get corrector as $u(s,t_1)$.
- For $r > 1$

  $\mathcal{L}(s,t_r) = 2g(u(s,t_{r-1}), {}^CD_s^{\gamma(s,t_{r-1})}u(s,t_{r-1})) - g(u(s,t_{r-2}), {}^CD_s^{\gamma(s,t_{r-2})}u(s,t_{r-2}))$,

  we get $u(s,t_r)$ by utilizing the linear interpolation between $u(s,t_{r-1})$ and $u(s,t_{r-2})$, $r = 2,3,\cdots,R$.

4 Analysis

This section focuses primarily on analyzing the proposed methods.

Theorem 1: *Error bound for the CAS wavelet series:*
Consider any differentiable function $u \in L^2[0,\eta]\times[0,T]$ *with the condition that* $\left|\frac{\partial^2}{\partial s^2}u\right| \le \varphi$, $\forall\ s \in [0,\eta]$, $t_r \in [0,T]$, *and* $\varphi > 0$. *Since the CAS wavelets are the basis of* $L^2[0,\eta]$, *any function* $u(s,t_r)$ *can be represented*

by the CAS wavelet series, $\sum_{p=0}^{\infty}\sum_{q\in\mathbf{Z}} l_{p,q}^{r}\psi_{p,q}(s)$*, and the series converges uniformly to* $u(s,t_r)$*. Furthermore, let* $u_{v,Q}(s,t_r)=\sum_{p=0}^{2^v-1}\sum_{q=-Q}^{Q} l_{p,q}^{r}\psi_{p,q}(s)$*, then*

$$|u(s,t_r)-u_{v,Q}(s,t_r)|\le \frac{\varphi}{\pi^2}\sum_{p=2^v}^{\infty}\sum_{q=Q+1}^{\infty}\frac{1}{(p+1)^{\frac{5}{2}}q^2}. \tag{26}$$

Proof. By following the same steps as given in [32], we can proof (26). □

From Eq. (26), we conclude that $\sum_{p=0}^{2^v-1}\sum_{q=-Q}^{Q} l_{p,q}^{r}\psi_{p,q}(s)$ converges to $u(s,t_r)$ for each $r=0,1,2,\cdots,R$, when $v,Q\to\infty$.

Theorem 2: *Convergence analysis for the CAS wavelet series*
Let v and Q approach to ∞*, then the series solution by the CAS wavelet method,* $u_{v,Q}(s,t_r)$*, converges to* $u(s,t_r)$ *for each* $r=0,1,2,\cdots,R$.

Proof. Let $H_{v,Q}^{r}(s)$ and $J_{v',Q'}^{r}(s)$ be the sequences of partial sums of $l_{p,q}^{r}\psi_{p,q}(s)$, such that

$$H_{v,Q}^{r}=\sum_{p=0}^{2^v-1}\sum_{q=-Q}^{Q} l_{p,q}^{r}\psi_{p,q}(s) \text{ and } J_{v',Q'}^{r}=\sum_{p=0}^{2^{v'}-1}\sum_{q=-Q'}^{Q'} l_{p,q}^{r}\psi_{p,q}(s), \text{ with } v>v' \text{ and } Q>Q'.$$

Let us have a set $A=[-Q,-Q+1,\cdots,-Q'-1,Q'+1,\cdots,Q]$. The orthogonal property of $\psi_{p,q}$ implies

$$\begin{aligned}\|H_{v,Q}^{r}(s)-J_{v',Q'}^{r}(s)\|^2 &= \|\sum_{p=2^{v'}}^{2^v-1}\sum_{q=A} l_{p,q}^{r}\psi_{p,q}(s)\|^2,\\ &= \langle\sum_{p=2^{v'}}^{2^v-1}\sum_{q=A} l_{p,q}^{r}\psi_{p,q}(s),\sum_{i=2^{v'}}^{2^v-1}\sum_{j=A} l_{i,j}^{r}\psi_{i,j}(s)\rangle,\\ &= \sum_{p=2^{v'}}^{2^v-1}\sum_{q=A} l_{p,q}^{r}\sum_{i=2^{v'}}^{2^v-1}\sum_{j=A}\overline{l_{i,j}^{r}}\langle\psi_{p,q}(s),\psi_{i,j}(s)\rangle,\\ &= \sum_{p=2^{v'}}^{2^v-1}\sum_{q=A}|l_{p,q}^{r}|^2.\end{aligned}$$

Since CAS wavelet forms an orthonormal basis of a Hilbert space $L^2[0,\eta]$, we have the following from the Bessel inequality

$$\sum_{p=0}^{\infty}\sum_{q\in\mathbf{Z}}|l_{p,q}^{r}|^2\le\|u(s,t_r)\|^2,$$

which implies $\sum_{p=0}^{\infty}\sum_{q\in\mathbf{Z}}|l_{p,q}^{r}|^2$ is convergent. Hence we have

$$\|H_{v,Q}^{r}(s)-J_{v',Q'}^{r}(s)\|^2\to 0 \quad \text{as} \quad v,v',Q,Q'\to\infty.$$

Thus $\{H^r_{v,Q}\}$ is a Cauchy sequence and it converges to say $g(s,t_r)$. Now we claim that $u(s,t_r)=g(s,t_r)$. For all $\psi_{i,j}$, we have

$$\begin{aligned}\langle g(s,t_r)-u(s,t_r),\psi_{i,j}(s)\rangle &= \langle g(s,t_r),\psi_{i,j}(s)\rangle - \langle u(s,t_r),\psi_{i,j}(\tau)\rangle,\\ &= \lim_{v,Q\to\infty}\langle H^r_{v,Q},\psi_{i,j}(s)\rangle - l^r_{i,j},\\ &= l^r_{i,j}-l^r_{i,j}=0.\end{aligned}$$

Hence $u(s,t_r)=g(s,t_r)$ and it completes the proof. □

Theorem 3. *[17] Let* $s_k=\eta\frac{2k-1}{2M}$, $k=1,2,\cdots,M$, $t_r=r\Delta t$, $r=0,1,2,\cdots,R\in\mathbb{N}$, $\Delta t=\frac{T}{R}$, *and* $\gamma^k_r=\gamma(s_k,t_r)$. *Suppose* $u(s_k,t)\in C^2[0,\eta]\times[0,t_r]$, *and define* ${}^{L1}\mathbb{E}^k_r={}^{C}D^{\gamma^k_r}_t u(s_k,t_r)-{}^{L1}D^{\gamma^k_r}_t u(s_k,t_r)$, *then we can conclude that*

$$\left|{}^{L1}\mathbb{E}^k_r\right|\le\frac{1}{\Gamma(2-\gamma^k_r)}\left[\frac{1-\gamma^k_r}{12}+\frac{2^{2-\gamma^k_r}}{2-\gamma^k_r}-(1+2^{-\gamma^k_r})\right]\max_{t_0\le t\le t_r}|\frac{\partial^2}{\partial t^2}u(s_k,t)|\Delta t^{2-\gamma^k_r}.$$

Theorem 4: *Suppose* $u(s_k,t)\in C^2[0,\eta]\times[0,t_r]$, *and define* ${}^{F}\mathbb{E}^k_r={}^{C}D^{\gamma^k_r}_t u(s_k,t_r)-{}^{F}D^{\gamma^k_r}_t u(s_k,t_r)$, *then we can conclude that*

$$\begin{aligned}\left|{}^{F}\mathbb{E}^k_r\right|\le{}&\frac{1}{\Gamma(2-\gamma^k_r)}\left[\frac{1-\gamma^k_r}{12}+\frac{2^{2-\gamma^k_r}}{2-\gamma^k_r}-(1+2^{-\gamma^k_r})\right]\max_{t_0\le t\le t_r}\left|\frac{\partial^2}{\partial t^2}u(s_k,t)\right|\Delta t^{2-\gamma^k_r}\\ &+\epsilon\,\frac{1}{\Gamma(2-\gamma^k_r)}\max_{t_0\le t\le t_{r-1}}\left|\frac{\partial}{\partial t}u(s_k,t)\right|t_r^{1-\gamma^k_r},\end{aligned}\tag{27}$$

where $\epsilon=\left(\frac{\Delta t}{T}\right)^2$.

Proof. We can proof (27) by using the theorem 3 and follow the same procedure given in [18]. □

From Theorem 3 and 4, we conclude that error from the $L1$ approximation and the fast algorithm are reducing while increasing the time steps, R. The order of the $L1$ approximation is $\left(2-\max_{0\le t\le T,0\le s\le\eta}\gamma(s,t)\right)$ and for fast algorithm is almost $\left(2-\max_{t_0\le t\le T,0\le s\le\eta}\gamma(s,t)\right)$.

For the L1 approximations of CVO time derivative, we need to store the values of all previous time levels when to compute it at the current time level. But, for the fast approximations of Caputo variable order derivative, we only require to compute $V_{k,r,i}$, since $V_{k,r-1,i}$ is already known at that time t_r.

5 Applications

In this section, we implement the L1-CAS and the fast-CAS method on the nonlinear multi-term CVO fractional partial differential equations.

5.1 Problem 1

Consider the nonlinear CVO fractional differential equation of the following form

$$\begin{aligned}{}^{C}D^{\gamma(s,t)}_t u(s,t)={}^{C}D^{\beta(s,t)}_s u(s,t)+u^2(s,t)+f(s,t),\ 1<\beta(s,t)\le 2,\ 0<\gamma(s,t)\le 1,\\ u(s,0)=s^2=u_0(s),\ 0\le s\le\eta,\\ u(0,t)=t^2=A_0(t),\ u(\eta,t)=\eta^2+t^2=C_0(t),\ 0\le t\le T,\end{aligned}\tag{28}$$

where $f(s,t) = \frac{\Gamma(3)}{\Gamma(3-\gamma(s,t))}t^{2-\gamma(s,t)} - \frac{\Gamma(3)}{\Gamma(3-\beta(s))}s^{2-\beta(s)} - s^4 - t^4 - (\sqrt{2}st)^2$. The exact solution of (28) is $u(x,t) = s^2 + t^2$. Let $\eta = T = 1$.

The purpose of Fig. 1 is to present a plot of the exact solution, $u_{ex}(s,t)$, approximate solution by the fast-CAS method, $u_{app}(s,t)$, and their corresponding absolute error. It shows that the solution by the fast-CAS method is in full agreement with the exact solution. For Table 1, we consider $\beta(s,t) = \frac{4-0.2e^{st}}{3}$, $\gamma(s,t) = 1 - 0.1\cos(st)$, $\nu = 2$, $Q = 2$, and different values of R. Tables 1 and 2 show that both the L1-CAS method and the fast-CAS method are almost equally accurate.

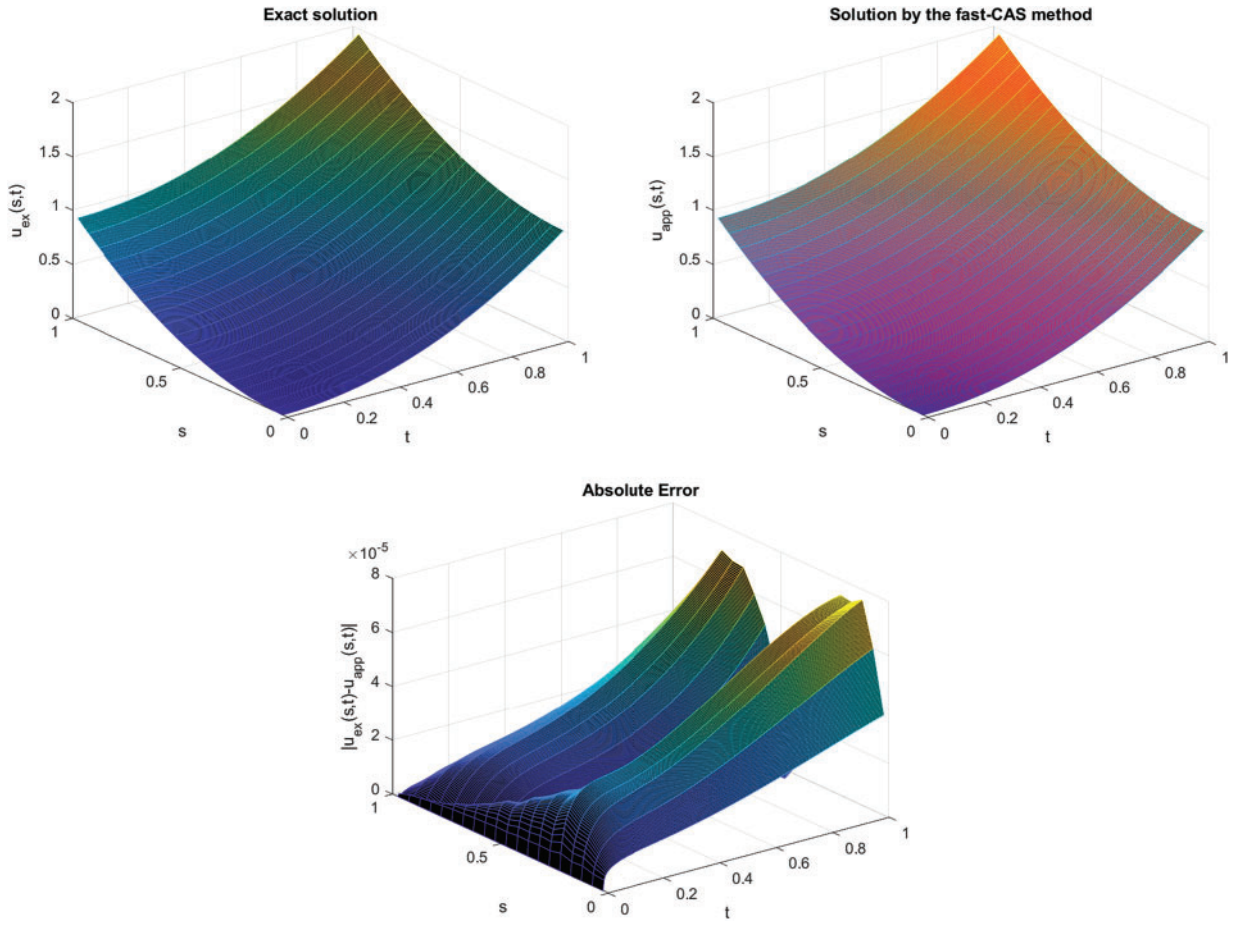

Figure 1: (Problem 1); Exact solution, solutions by the fast-CAS method ($\nu = 2$, $Q = 2$ and $R = 250$) and their corresponding absolute error

Since the maximum value of $\gamma(s,t) = 1 - 0.1\cos(st)$ is approximately 0.946, the truncation error is around 1.054. Table 1 demonstrates that the Theorem 3 and 4 are valid. It is worth noting that if β is the function of two variables s and t, then we have to regenerate the operational matrices $\boldsymbol{F}_{M\times M}^{\beta(s,t_r)}$, for each time step t_r, $r = 0, 1, 2, \cdots, R \in \mathbb{N}$. But, if β is only the function of s, then there is no need to regenerate the operational matrices at each time step. This is the reason that the proposed methods take much time when β is the function of both s and t, which can be observed in Tables 1 and 2. Both tables also show that error reduces while increasing the number of time steps, R, level of resolution, ν, and order of CAS wavelet, Q, as given in the Theorems 1, 2, 3 and 4 of Section 4.

Table 1: (Problem 1); Comparison of the fast-CAS method and the L1-CAS method when $\beta(s,t) = \frac{4-0.2e^{st}}{3}$, $\gamma(s,t) = 1 - 0.1\cos(st)$, $v = 2$, $Q = 2$, and for different values of time steps, R

Time steps	The fast-CAS method CPU time (sec)			The L1-CAS method CPU time (sec)		
R	E_{fast}	CPU_{fast}	Order	E_{L1}	CPU_{L1}	Order
128	4.2824×10^{-4}	3.8685	–	4.2811×10^{-4}	6.3735	–
256	2.2756×10^{-4}	7.6604	0.9122	2.2755×10^{-4}	12.7295	0.9118
512	1.1492×10^{-4}	20.1958	0.9856	1.1492×10^{-4}	27.7984	0.9856
1024	5.6662×10^{-5}	25.4031	1.0202	5.6662×10^{-5}	91.9092	1.0202
2048	2.7604×10^{-5}	52.0936	1.0375	2.7604×10^{-5}	168.2688	1.0375
4096	1.3407×10^{-5}	106.5251	1.0419	1.3407×10^{-5}	392.0936	1.0419
8192	6.4980×10^{-6}	201.4929	1.0449	6.4980×10^{-6}	919.8896	1.0449
16384	3.1425×10^{-6}	520.6885	1.0481	3.1425×10^{-6}	1917.2081	1.0481
32768	1.5175×10^{-6}	830.6178	1.0502	1.5175×10^{-6}	9358.9488	1.0502

Table 2: (Problem 1); Comparison of the fast-CAS method and the L1-CAS method when $\gamma(s,t) = \frac{3(1+\sin(\frac{t}{2}))+0.01\cos(s)}{7}$, $\beta(s,t) = \frac{4-0.2e^{s}}{3}$, and for different values of time and space steps

Time steps	Space steps	The fast-CAS method	CPU time (sec)	The L1-CAS method	CPU time (sec)
R	$M = 2^v(2Q+1)$	E_{fast}	CPU_{fast}	E_{L1}	CPU_{L1}
400	$v = 1,\ Q = 1$	6.2659×10^{-6}	0.4921	6.2455×10^{-6}	0.6997
800		3.9387×10^{-6}	0.8257	3.9377×10^{-6}	2.2560
1600		1.9070×10^{-6}	1.5082	1.9068×10^{-6}	8.1965
3200		8.3608×10^{-7}	3.3498	8.3561×10^{-7}	49.5519
6400		3.4952×10^{-7}	7.3480	3.4950×10^{-7}	193.0405
12800		1.4338×10^{-7}	15.9716	1.4338×10^{-7}	891.0754
400	$v = 3,\ Q = 3$	4.6879×10^{-6}	1.0557	4.6725×10^{-6}	2.3846
800		3.0036×10^{-6}	1.8772	3.0028×10^{-6}	14.9820
1600		1.4757×10^{-6}	3.7230	1.4755×10^{-6}	92.3427
3200		6.4982×10^{-7}	7.8293	6.4946×10^{-7}	349.0080
6400		2.7111×10^{-7}	27.6802	2.7109×10^{-7}	809.6388
12800		1.1002×10^{-7}	50.0747	1.1002×10^{-7}	3470.0805

For Fig. 2, we utilize $\beta(s,t) = \frac{2.9-0.1\sin(s)+\cos(s)}{3}$, $\gamma(s,t) = \frac{3(1+\sin(\frac{t}{2}))+0.01\cos(s)}{7}$, $R = 50$, and different values of v and Q. It shows that the maximum absolute error by the fast-CAS wavelet method reduces while increasing the value of parameters v and Q, as given in Theorems 1 and 2.

The computational cost is assessed by measuring the CPU time required for the fast-CAS and L1-CAS methods against the total number of time steps R, with $v = 1$ and $Q = 1$ fixed, as shown in Fig. 3 and Table 2. For Fig. 3, we consider $R = 400 \times 2^n$, $n = 0, 1, 2, 3, 4, 5$, and use the values of n on the x–$axis$ instead of $\log_{10}(R)$. It indicates that the CPU consumption rate of the fast-CAS method and the L1-CAS method is approximately $O(R)$ and $O(R^2)$, respectively.

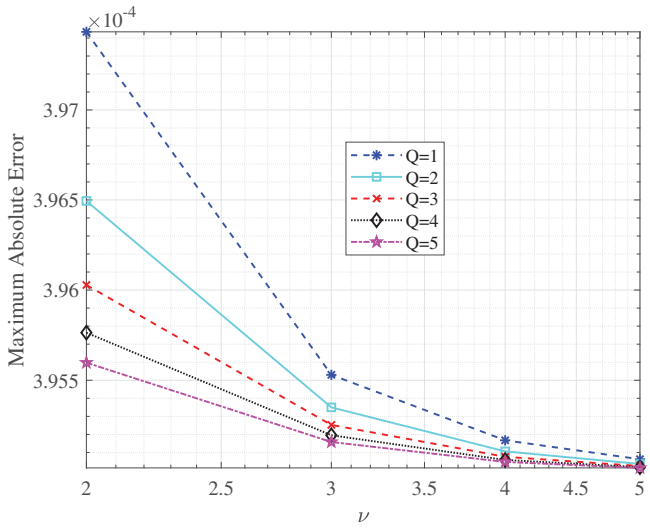

Figure 2: **(Problem 1)**; The maximum absolute errors by the fast-CAS method for $R = 50$, and different values of Q and ν

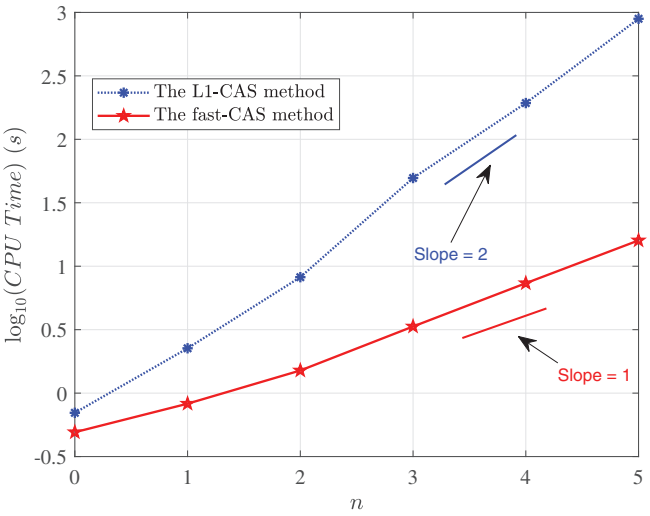

Figure 3: **(Problem 1)**; Comparison of the fast-CAS and the L1-CAS method are presented for $Q = 1$, $\nu = 1$ and at different values of time steps R

5.2 Problem 2

Consider the following nonlinear multi-term CVO fractional Burger's type equation of the form

$$\begin{aligned} {}^{C}D_{t}^{\gamma(s,t)}u(s,t) + u(s,t)\,{}^{C}D_{s}^{\alpha(s)}u(s,t) &= a_1(s,t)\,{}^{C}D_{s}^{\beta_1(s,t)}u(s,t) \\ &+ a_2(s,t)\,{}^{C}D_{s}^{\beta_2(s,t)}u(s,t) + f(s,t), \\ u(s,0) = s^{\xi} = u_0(s),\ 0 \le s \le \eta,& \\ u(0,t) = t^{\chi} = A_0(t),\ u(\eta,t) = \eta^{\xi} + (1+2\eta^{\xi})t^{\chi} = C_0(t),\ 0 \le t \le T,& \end{aligned} \tag{29}$$

where $a_1(s,t) = 2e^{\sin(s)} + 4t,\ a_2(s,t) = 2\sin(s) + 5e^t,\ 1 < \beta_1(s,t) < 2,\ 0 < \beta_2(s,t) < 1,\ 0 < \gamma(s,t) < 1,\ 0 < \alpha(s) < 1$, and

$$f(s,t) = (1+2s^{\xi})\frac{\Gamma(\chi+1)}{\Gamma(\chi+1-\gamma(s,t))}t^{\chi-\gamma(s,t)} + (1+2t^{\chi})(s^{\xi}+t^{\chi}+2s^{\xi}t^{\chi})\frac{\Gamma(\xi+1)}{\Gamma(\xi+1-\alpha(s))}s^{\xi-\alpha(s)}$$
$$- a_1(s,t)(1+2t^{\chi})\frac{\Gamma(\xi+1)}{\Gamma(\xi+1-\beta_1(s,t))}s^{\xi-\beta_1(s,t)} - a_2(s,t)(1+2t^{\chi})\frac{\Gamma(\xi+1)}{\Gamma(\xi+1-\beta_2(s,t))}s^{\xi-\beta_2(s,t)}.$$

The exact solution of (29) is $u(x,t) = s^{\xi} + t^{\chi} + 2s^{\xi}t^{\chi}, \xi,\ \chi \in \mathbb{R}$. Let $\eta = T = 1$.

For Fig. 4, we utilize the following values of the parameters $\chi = 5.96,\ \xi = 3.67,\ \gamma(s,t) = \frac{3+\sin(\frac{t}{2})+\cos(s)}{5},\ \beta_1(s,t) = \frac{4-0.2e^s}{3},\ \beta_2(s,t) = 1.3 - e^{-x},\ \alpha(s) = \frac{2-e^{-s}}{3},\ R = 150, \nu = 3, Q = 3$. The purpose of Fig. 4 plots the exact solution, $u_{ex}(s,t)$, approximate solution by the fast-CAS method, $u_{app}(s,t)$, and their corresponding absolute error. It shows that the solution by the fast-CAS method is in full agreement with the exact solution. Table 3 demonstrates that both the fast-CAS method and the L1-CAS methods are nearly equally accurate. However, the fast-CAS method significantly reduces computational time compared to the L1-CAS method, fulfilling its primary objective. Table 3 also shows that error reduces while increasing the number of time steps, R, level of resolution, ν, and order of CAS wavelet, Q, as given in the Theorems 1, 2, 3 and 4 of Section 4.

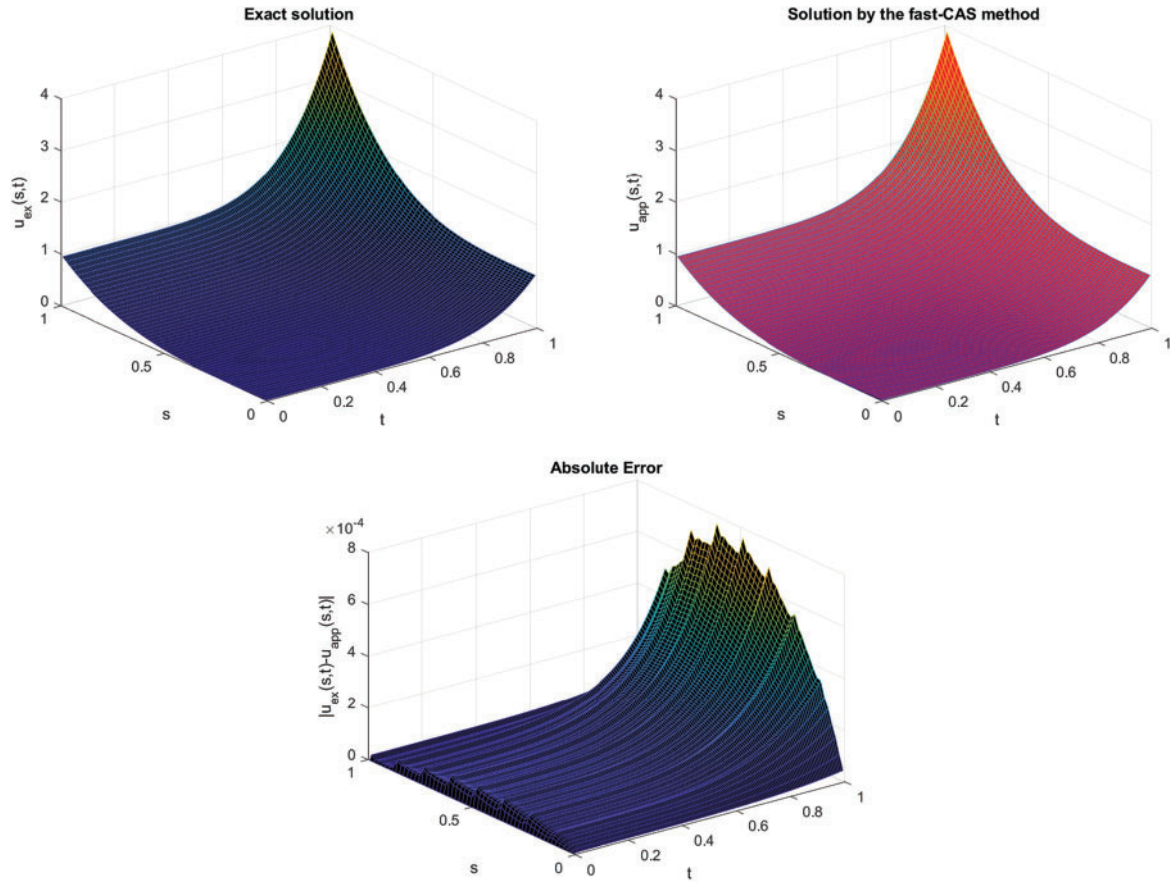

Figure 4: (Problem 2); Exact solution, solutions by the fast-CAS method ($\nu = 3,\ Q = 3$ and $R = 150$) and their corresponding absolute error

Table 3: (Problem 2); Comparison of the fast-CAS method and the L1-CAS method when $\gamma(s,t) = \frac{3+\sin(\frac{t}{2})+\cos(s)}{5}$, $\beta_1(s,t) = \frac{4-0.2e^s}{3}$, $\beta_2(s,t) = 1.3 - e^{-x}$, $\alpha(s) = \frac{2-e^{-s}}{3}$, and for different values of time and space steps

Time steps R	Space steps $M = 2^v(2Q+1)$	The fast-CAS method E_{fast}	CPU time (sec) CPU_{fast}	The L1-CAS method E_{L1}	CPU time (sec) CPU_{L1}
500	$v = 1,\ Q = 1$	2.3296×10^{-2}	0.5900	2.3296×10^{-2}	0.8353
1000	$v = 2,\ Q = 2$	1.9067×10^{-3}	1.0206	1.9067×10^{-3}	5.9062
2000	$v = 3,\ Q = 3$	2.4089×10^{-4}	3.1208	2.4089×10^{-4}	85.9915
4000	$v = 4,\ Q = 4$	4.1563×10^{-5}	42.0548	4.1563×10^{-5}	447.4726
8000	$v = 5,\ Q = 5$	8.8923×10^{-6}	328.8019	8.8923×10^{-6}	4240.1071

For Fig. 5, we utilize $\beta_1(s,t) = 2 - e^{-0.2s}$, $\beta_2(s,t) = 1 - e^{-0.2s}$, $\gamma(s,t) = \frac{2.1+\sin(t)+\cos(s)}{4}$, $\alpha(s) = 1.5 - e^{-0.2s}$, $R = 500$, $\chi = 2$, $\xi = 2$, and different values of v and Q. It shows that the solution by the fast-CAS wavelet method converges to the exact solution while increasing the number of values of v and Q, as given in Theorems 1 and 2. For $\gamma(s,t) = -0.2\log(st+1) + 0.8$, Table 4 is used to enlist the maximum absolute error and the order of convergence for the fast-CAS wavelet method at $v = 2$, $Q = 2$, and for different values of R. Since the maximum value of $\gamma(s,t)$ is 0.8, the truncation error is approximately $2 - 0.8 = 1.2$, which is consistent with Theorems 3 and 4.

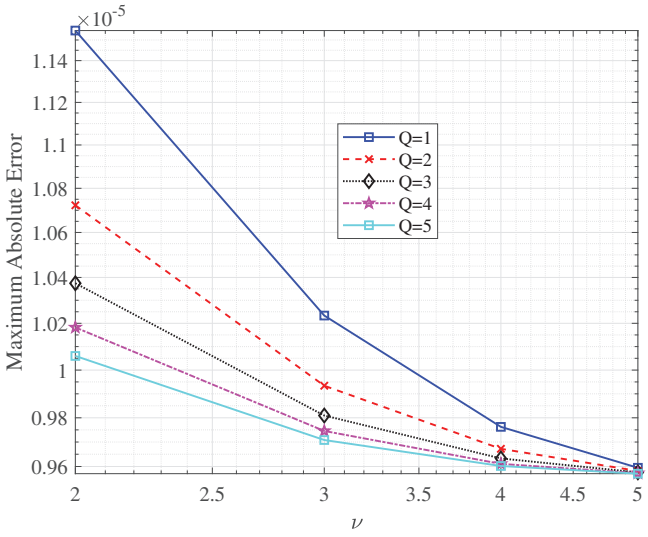

Figure 5: (Problem 2); The maximum absolute errors by the fast-CAS method for $R = 500$, and different values of Q and v

For Fig. 6, we consider $\gamma(s,t) = \frac{2+\sin(t)+\cos(s)}{4}$, $\beta_1(s,t) = \frac{4-0.2e^s}{3}$, $\beta_2(s,t) = 1.3 - e^{-x}$, $\alpha(s) = 1.3 - e^{-x}$, $\chi = 1$, $\xi = 2$. The computational cost is assessed by measuring the CPU time required for the fast-CAS and L1-CAS methods against the total number of time steps R, with $v = 2$ and $Q = 2$ fixed, as shown in Fig. 6. For Fig. 6, we consider $R = 400 \times 2^n$, $n = 0, 1, 2, 3, 4, 5$, and use the values of n on the $x - axis$ instead of $\log_{10}(R)$. Fig. 6 shows that the rate of CPU time for the L1-CAS method is around 2 and for the fast-CAS method is around 1. It means that the fast-CAS method is more efficient as compared to the L1-CAS method.

Table 4: (Problem 2); The maximum error and order of convergence at $\nu = 2,\ Q = 2$, and for different values of time steps, R

Time steps R	Error $\gamma(s,t) = -0.2\log(st+1) + 0.8$	Order
256	3.8538×10^{-5}	–
512	1.6497×10^{-5}	1.2241
1024	7.0865×10^{-6}	1.2191
2048	3.0514×10^{-6}	1.2156
4096	1.3176×10^{-6}	1.2115
8192	5.7042×10^{-7}	1.2078
16384	2.4770×10^{-7}	1.2034

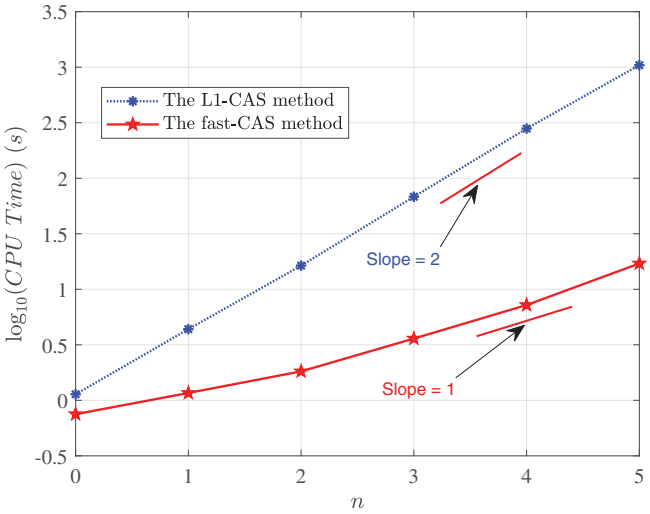

Figure 6: (Problem 2); Comparison of the fast-CAS and the L1-CAS method are presented for $Q = 2$, $\nu = 2$ and at different values of timesteps R

5.3 Problem 3

Consider the nonlinear CVO fractional differential equation of the following form

$$\begin{aligned} &{}^{C}D_{t}^{\gamma(s,t)}u(s,t) = {}^{C}D_{s}^{\beta(s,t)}u(s,t) + \sin(u)^{\zeta} + f(s,t),\ 1 < \beta(s,t) \le 2,\ 0 < \gamma(s,t) \le 1, \\ &u(s,0) = \sin(s),\ 0 \le s \le \eta, \\ &u(0,t) = 0, u(\eta,t) = \sin(\eta) + cos(t),\ 0 \le t \le T, \end{aligned} \tag{30}$$

where

$$f(s,t) = -\sin(s)t^{2-\gamma(s,t)}E_{2,3-\gamma(s,t)}(-t^2) + \cos(t)s^{3-\beta(s,t)}E_{2,4-\beta(s,t)}(-s^2) - \sin\left(\sin(s)\cos(t)\right)^{\xi},$$

$\xi \in \mathbb{R}^{+}$ and $E_{a,b}(s)$ is the two parameter Mittag-Leffler function [37]. The exact solution of (30) is $u(s,t) = \sin(s)\cos(t)$. We have considered $\xi = 3.75,\ \gamma(s,t) = \frac{2+\sin(t)+\cos(t)}{4}$, and $\beta(s,t) = \frac{4-0.2e^{st}}{3}$. The purpose of Fig. 7 plots the exact solution, $u_{ex}(s,t)$, approximate solution by the fast-CAS method (when $\nu = Q = 3,\ R = 200$), $u_{app}(s,t)$, and their corresponding absolute error. It shows that the solution by the

fast-CAS method is in full agreement with the exact solution. For $\gamma(s,t) = \frac{2+\sin(t)+\cos(t)}{4}$, Table 5 is used to enlist the maximum absolute error and the order of convergence for the fast-CAS wavelet method at $v = 3$, $Q = 3$, and for different values of R. Since the maximum value of $\gamma(s,t)$ is approximately 0.96, the truncation error is approximately 1.0397, which is consistent with Theorems 3 and 4. For Fig. 8, we consider $R = 400 \times 2^n$, $n = 2,3,4,5,6$ and use the values of n on the $x - axis$ instead of $\log_{10}(R)$. Fig. 8 shows that the rate of CPU time for the L1-CAS method is around 2 and for the fast-CAS method is around 1. It means that the fast-CAS method is more efficient as compared to the L1-CAS method.

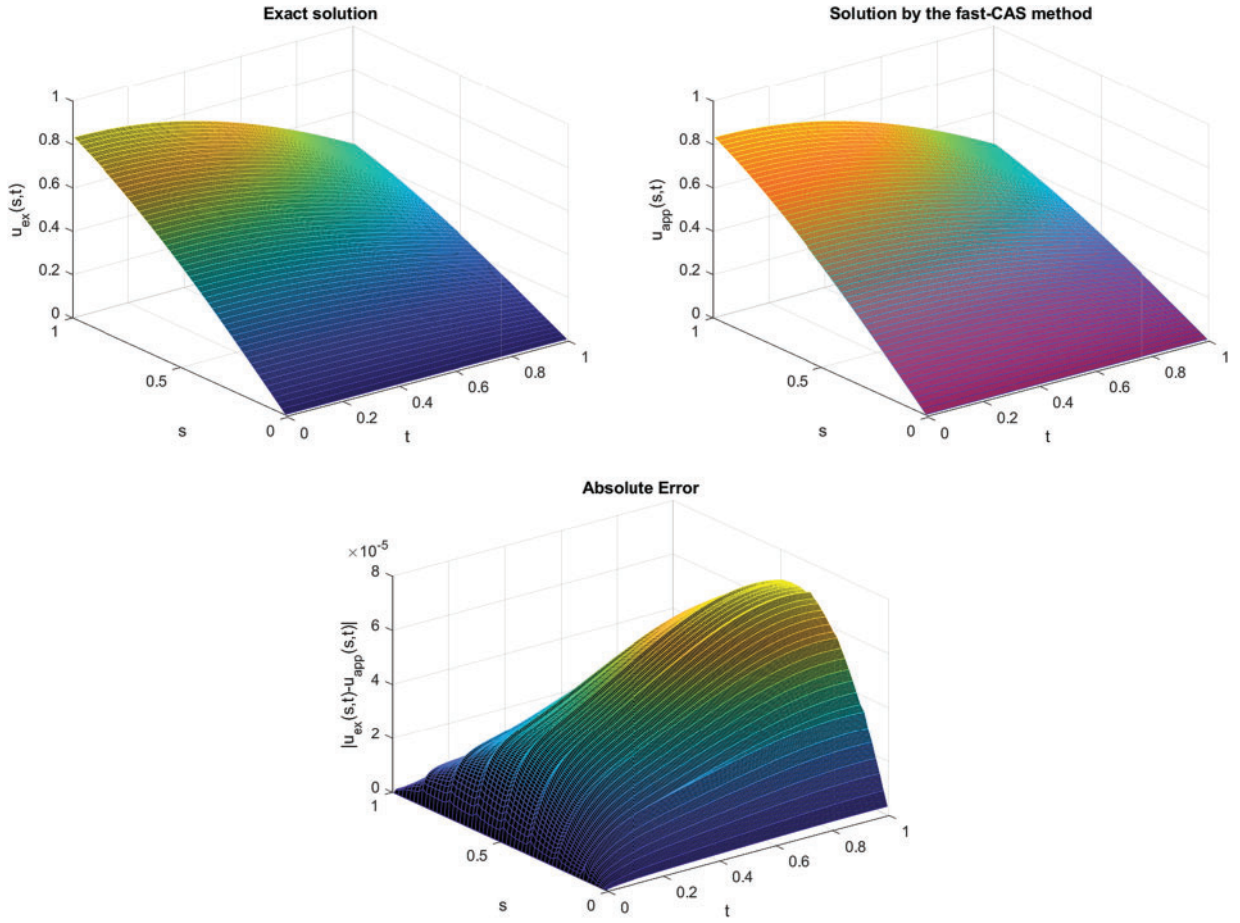

Figure 7: (Problem 3); Exact solution, solutions by the fast-CAS method ($v = 3$, $Q = 3$ and $R = 200$) and their corresponding absolute error

Table 5: (Problem 3); The maximum error and order of convergence at $v = 3$, $Q = 3$, and for different values of time steps, R

Time steps R	The fast-CAS method E_{fast}	Order
16	1.5105×10^{-3}	–
32	6.2485×10^{-4}	1.2735
64	2.6972×10^{-4}	1.2121

(Continued)

Table 5 (continued)

Time steps R	The fast-CAS method E_{fast}	Order
128	1.1914×10^{-4}	1.1787
256	5.3325×10^{-5}	1.1599
512	2.5050×10^{-5}	1.0900
1024	1.2309×10^{-5}	1.0251

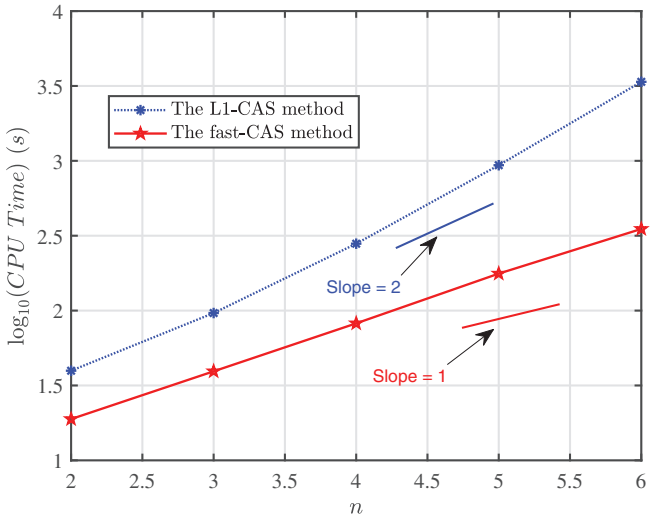

Figure 8: (Problem 3); Comparison of the fast-CAS and the L1-CAS method are presented for $Q = 1$, $\nu = 1$ and at different values of timesteps R

6 Conclusion

This research paper makes two significant contributions to the existing literature. First, it introduces two novel methods, the L1-CAS and the fast-CAS, specifically designed for multiterm Caputo variable-order (CVO) fractional partial differential equations. Second, it combines these two methods with an interpolation technique, which has proven particularly effective for solving nonlinear multiterm CVO fractional partial differential equations. We have successfully derived the CAS wavelet operational matrix of variable-order fractional integration and applied it to boundary value problems. The implementation procedures of both methods are discussed in detail, and their pseudo codes are also provided. Numerical simulations are conducted to illustrate the theoretical results, and the findings are presented through both tabular and graphical formats. Separate truncation error estimates for temporal and spatial discretizations are given; however, a full space-time convergence analysis remains an open problem to be addressed in future work.

The results, including Figs. 1, 4, and 7, demonstrate that the fast-CAS method produces solutions in complete agreement with the exact solutions. Tables 1 to 5 and Figs. 2 and 5 show that the maximum absolute error decreases as the parameters ν, Q, and R increase, consistent with the theoretical analysis. Furthermore, as shown in Tables 1, 4, and 5, both proposed methods achieve the same order of convergence as established in Theorems 3 and 4 of Section 4. The CPU time results in Figs. 3, 6, and 8 indicate that the L1-CAS method

scales with a rate around 2, while the fast-CAS method scales with a rate around 1, confirming that the fast-CAS method is more efficient.

Although the CAS wavelet operational matrix method is accurate, it demands significant computational time, especially for large ν and Q values, due to the increased size of operational matrices. In contrast, both L1-CAS and fast-CAS methods maintain similar levels of accuracy with reduced computational cost. Notably, the fast-CAS method is the most efficient. Moreover, these methods can be readily extended to higher-dimensional linear and nonlinear multiterm CVO partial differential equations, for which the traditional CAS wavelet method becomes computationally intensive.

Acknowledgement: Not applicable.

Funding Statement: This work was supported by the National Research Foundation of Korea (NRF) grant funded by the Korean government (MSIT) (NRF-2021R1A2C1011817) and the BK21 Program (Next Generation Education Program for Mathematical Sciences, 4299990414089) funded by the Ministry of Education (MOE, Republic of Korea).

Author Contributions: The authors confirm their contribution to the paper as follows: Junseo Lee: Formal analysis, software, methodology, data collection, visualization. Bongsoo Jang: Conceptualization, supervision, resources, funding acquisition. Umer Saeed: Conceptualization, formal analysis, methodology, validation. All authors reviewed the results and approved the final version of the manuscript.

Availability of Data and Materials: The datasets generated or analyzed during the current study are available from the corresponding author on reasonable request.

Ethics Approval: Not applicable.

Conflict of Interest: The authors declare no conflicts of interest to report regarding the present study.

References

1. Awati VB, Goravar A, Kumar M. Spectral and Haar wavelet collocation method for the solution of heat generation and viscous dissipation in micro-polar nanofluid for MHD stagnation point flow. Math Comput Simul. 2024;215:158–83. doi:10.1016/j.matcom.2023.07.031.
2. Rabiei K, Razzaghi M. An approach to solve fractional optimal control problems via fractional-order Boubaker wavelets. J Vib Control. 2022;29(7–8):1806–19. doi:10.1177/10775463211070902.
3. Agrawal K, Kumar R, Kumar S, Hadid S, Momani S. Bernoulli wavelet method for non-linear fractional Glucose–Insulin regulatory dynamical system. Chaos Soliton Fract. 2022;164(5):112632. doi:10.1016/j.chaos.2022.112632.
4. Faheem M, Raza A, Khan A. Collocation methods based on Gegenbauer and Bernoulli wavelets for solving neutral delay differential equations. Math Comput Simul. 2021;180(26):72–92. doi:10.1016/j.matcom.2020.08.018.
5. Saeed U. A method for solving Caputo-Hadamard fractional initial and boundary value problems. Math Methods Appl Sci. 2023;46(13):13907–21. doi:10.1002/mma.9297.
6. Saeed U, Rehman M. Haar wavelet-quasilinearization technique for fractional nonlinear differential equations. Appl Math Comput. 2013;220(1):630–48. doi:10.1016/j.amc.2013.07.018.
7. Saeed U, Idrees S, Javid K, Din Q. Krawtchouk wavelets method for solving Caputo and Caputo-Hadamard fractional differential equations. Math Methods Appl Sci. 2022;45(17):11331–54. doi:10.1002/mma.8452.
8. Hedayati M, Ezzati R, Noeiaghdam S. New procedures of a fractional order model of novel coronavirus (COVID-19) outbreak via wavelets method. Axioms. 2021;10(2):122. doi:10.3390/axioms10020122.
9. Hedayati M, Ezzati R. A new operational matrix method to solve nonlinear fractional differential equations. Nonlinear Eng. 2024;13(1):20220364. doi:10.1515/nleng-2022-0364.
10. Khan NA, Altaf S, Khan NA, Ayaz M. Haar wavelet Arctic Puffin optimization method (HWAPOM): application to logistic models with fractal-fractional Caputo-Fabrizio operator. Partial Differ Equ Appl Math. 2025;13(2):101114. doi:10.1016/j.padiff.2025.101114.

11. Khan NA, Ali M, Ara A, Khan MI, Abdullaeva S, Waqas M. Optimizing pantograph fractional differential equations: a Haar wavelet operational matrix method Partial. Differ Equ App Math. 2024;11(7):100774. doi:10.1016/j.padiff.2024.100774.
12. Nemati S, Lima PM, Torres DFM. Numerical solution of variable-order fractional differential equations using Bernoulli polynomials. Fractal Fract. 2021;5(4):219. doi:10.3390/fractalfract5040219.
13. Chen YM, Wei YQ, Liu DY, Yu H. Numerical solution for a class of nonlinear variable order fractional differential equations with Legendre wavelets. Appl Math Lett. 2015;46(2):83–8. doi:10.1016/j.aml.2015.02.010.
14. Kanwal A, Boulaaras S, Shafqat R, Taufeeq B, Rahman M. Explicit scheme for solving variable-order time-fractional initial boundary value problems. Sci Rep. 2024;14(1):5396. doi:10.1038/s41598-024-55943-4.
15. Guo Y, Ye G. Existence and uniqueness of weak solutions to variable-order fractional Laplacian equations with variable exponents. J Funct Spaces. 2021;2021(3):6686213. doi:10.1155/2021/6686213.
16. Tajadodi H. Variable-order Mittag-Leffler fractional operator and application to mobile-immobile advection-dispersion model. Alex Eng J. 2022;61(5):3719–28. doi:10.1016/j.aej.2021.09.007.
17. Shen S, Liu F, Chen J, Turner I, Anh V. Numerical techniques for the variable order time fractional diffusion equation. Appl Math Comput. 2012;218(22):10861–70. doi:10.1016/j.amc.2012.04.047.
18. Zhang JL, Fang ZW, Sun HW. Exponential-sum-approximation technique for variable-order time-fractional diffusion equations. J Appl Math Comput. 2021;68(1):323–47. doi:10.1007/s12190-021-01528-7.
19. Zhang J, Fang ZW, Sun HW. Robust fast method for variable-order time-fractional diffusion equations without regularity assumptions of the true solutions. Appl Math Comput. 2022;430:127273. doi:10.1016/j.amc.2022.127273.
20. Fang ZW, Sun HW, Wang H. A fast method for variable-order Caputo fractional derivative with applications to time-fractional diffusion equations. Comput Math Appl. 2020;80(5):1443–58. doi:10.1016/j.camwa.2020.07.009.
21. Zhang L, Zhang GF. Fast algorithms for high-dimensional variable-order space-time fractional diffusion equations. Comput Appl Math. 2021;40(4):116. doi:10.1007/s40314-021-01496-5.
22. Dehestani H, Ordokhani Y, Razzaghi M. A novel direct method based on the Lucas multiwavelet functions for variable-order fractional reaction-diffusion and subdiffusion equations. Numer Linear Algebra Appl. 2021;28(2):e2346. doi:10.1002/nla.2346.
23. Heydari MH, Avazzadeh Z, Razzaghi M. Vieta-Lucas polynomials for the coupled nonlinear variable-order fractional Ginzburg-Landau equations. Appl Numer Math. 2021;165(2):442–58. doi:10.1016/j.apnum.2021.03.007.
24. Hosseininia M, Heydari MH, Avazzadeh Z. A hybrid wavelet-meshless method for variable-order fractional regularized long-wave equation. Eng Anal Bound Elem. 2022;142(1):61–70. doi:10.1016/j.enganabound.2022.05.021.
25. Jia J, Wang H, Zheng X. A fast algorithm for time-fractional diffusion equation with space-time-dependent variable order. Numer Algorithms. 2023;94(4):1705–30. doi:10.1007/s11075-023-01552-7.
26. Dehestani H, Ordokhani Y, Razzaghi M. Pseudo-operational matrix method for the solution of variable-order fractional partial integro-differential equations. Eng Comput. 2021;37(3):1791–806. doi:10.1007/s00366-019-00912-z.
27. Dehestani H, Ordokhani Y, Razzaghi M. Application of the modified operational matrices in multiterm variable-order time-fractional partial differential equations. Math Methods Appl Sci. 2019;42(18):7296–7313. doi:10.1002/mma.5840.
28. Biswas C, Das S, Singh A, Altenbach H. Solution of variable-order partial integro-differential equation using Legendre wavelet approximation and operational matrices. Z Angew Math Mech. 2023;103(2):e202200222. doi:10.1002/zamm.202200222.
29. Heydari MH, Cattani C, Hooshmandasl MR, Hariharan G. An optimization wavelet method for multi variable-order fractional differential equations. Fundam Inform. 2017;151(1–4):255–73. doi:10.3233/FI-2017-1491.
30. Shah K, Naz H, Sarwar M, Abdeljawad T. On spectral numerical method for variable-order partial differential equations. AIMS Math. 2022;7(6):10422–38. doi:10.3934/math.2022581.
31. Yousefi S, Banifatemi A. Numerical solution of Fredholm integral equations by using CAS wavelets. Appl Math Comput. 2006;183(1):458–63. doi:10.1016/j.amc.2006.05.081.
32. Saeed U. CAS Picard method for fractional nonlinear differential equation. Appl Math Comput. 2017;307(1):102–12. doi:10.1016/j.amc.2017.02.044.

33. Beylkin G, Monzón L. Approximation by exponential sums revisited. Appl Comput Harmon Anal. 2010;28(2):131–49. doi:10.1016/j.acha.2009.08.011.
34. Yi H, Chen Y, Wang Y, Huang Y. Optimal convergence analysis of a linearized second-order BDF-PPIFE method for semi-linear parabolic interface problems. Appl Math Comput. 2023;438(3):127581. doi:10.1016/j.amc.2022.127581.
35. Bellman RE, Kalaba RE. Quasilinearization and nonlinear boundary-value problems. New York, NY, USA: American Elsevier Publishing Company; 1965. doi:10.2307/3612757.
36. Cherruault Y. Convergence of Adomian's method. Math Comput Model. 1990;14:83–6. doi:10.1016/0895-7177(90)90152-D.
37. Mittag-Leffler GM. Sur la nouvelle fonction $E_{\alpha}(x)$. Comptes Rendus de l′ Académie Des Sciences. 1903;137:554–8.